Digest Journal of Nanomaterials and Biostructures Vol. 15, No. 4, October-December 2020, p.1215-1226

AN AB INITIO INVESTIGATION OF THE EFFECT OF Co, Ru, W, Ta ON THE STABILITY AND ELECTRONIC PROPERTIES OF Ni–BASE SINGLE CRYSTAL SUPERALLOYS

J. LIU[a], X. DU[b*], J. LI[a]

[a]*Institute of Metal Research, Chinese Academy of Sciences, Shenyang, 110016, PR China*

[b]*School of Materials Science and Engineering, Shenyang Ligong University, Shenyang 110159, PR China*

A first principles calculation method was used to investigate the site preference of Co, Ru, W, Ta at the γ'/γ interface in Ni-based single-crystal superalloys. The calculation results show that the addition of Co, Ru, W and Ta can decrease the total energy and the binding energy of γ'/γ interface, which may result in an improved microstructure stability of Ni-based single-crystal superalloys. Cr atom prefers to occupy a Ni site in γ phase, while Ru, W and Ta atoms prefer to occupy Al sites in γ' phase. It is found that the electronic bonding mechanism of γ'/γ interface with the doped alloying elements can be summarized as the combination of d-d hybridization between Co-3d, d-p hybridization among Ru-4d, W-5d, Ta-5d orbits located at Al4 site in γ' phase and Al-3p orbits and the electron charge transfers from Cr, Ru, W and Ta to Ni sites. The enhanced chemical bondings between alloying atoms and their neighbor host atoms are considered to be the main strengthening mechanism of the alloying elements in γ'/γ interface of Ni-based single-crystal superalloys.

(Received June 22, 2020; Accepted December 11, 2020)

Keywords: Site occupancy, Ab initio calculations, Ni-based single crystal superalloys, Electronic structure

1. Introduction

Nickel-based single crystal superalloys, which have become the most widely used alloys for high temperature applications, such as for the turbine blades and vanes in modern aero-engines, are characterized by a high volume fraction of cuboidal γ'- Ni_3Al phase precipitates coherently embedded in the γ-Ni matrix phase [1]. γ'- Ni_3Al phase is the key strengthening component of the commercial Ni-base superalloys for high-temperature applications. Various studies have shown that the high temperature creep rupture strength, thermal fatigue resistance, and oxidation resistance of γ'-Ni3Al can be significantly improved by the addition of increasing amount of refractory elements [2-13]. These elements are effective in improving the solution strengthening effect and the elevated temperature strength of Ni-based superalloys [14,15]. The refractory elements content has increased from ~14 wt.% for first-generation (CMSX-2) superalloys to

*Corresponding author: du511@163.com

greater than 20 wt.% for third-generation (CMSX-10) superalloys [16]. The behavior and properties of these metals in Ni_3Al has been extensively explored in recent studies both experimentally and computationally. For example, Cr is responsible for improving the elastic strength as well as providing oxidation resistance [17]. W provides solid solution strengthening [18], and Re improves creep resistance [19]. Ru is proven to be an effective element that can suppress the formation of topologically close-packed (TCP) phases in superalloys [20–22]. The partitioning behavior of refractory elements in Ni-based superalloys has been extensively investigated [23–30]. However, to the author's best knowledge, there is no report on theoretical studies of the effect of refractory elements on the stability of Ni_3Al /Ni interface and Ni matrix. Further advances in single-crystal superalloys require a thorough understanding of the strengthening mechanisms of refractory elements in Ni_3Al /Ni interface.

In the present work, the site preferences of 3d, 4d, 5d refractory elements (Co, Ru, W and Ta) in γ-Ni and γ'- Ni_3Al phase of Ni-based superalloy are systematically studied using first-principles calculations. Our work provides a theoretical basis for further insight into the role of refractory elements in controlling the mechanical properties of Ni-based superalloys.

2. Method and computational model

The energetic and electronic structures as well as the geometric characteristics of the γ/γ' interface with addition of refractory elements were performed by using the first principles calculations based on density functional theory (DFT) [31] implemented in Quantum-ESPRESSO program package [32]. Meanwhile, The Perdew-Burke-Ernzerhof (PBE) exchange correlation functional within generalized gradient approximation(GGA) is taken into account. The Monkhorst-Pack scheme [33] was used for k point sampling in the first irreducible Brillouin zone (BZ). The k points separation in the Brillouin zone of the reciprocal space were 4×4×2. The cutoff energy for plane wave expansions was determined as 540 eV after convergence tests. The convergence criteria for geometry optimization were as follows: electronic self-consistent field (SCF) tolerance less than 5.0×10-5 eV/atom, Hellmann–Feynman force below 0.01eV/Å, maximum stress less than 0.05GPa and displacement within 2.0×10-4 Å.

A supercell model of γ/γ' interface, which consists of 64 atoms and two γ/γ' interfaces, is devised for the present study. The atomic arrangement of the γ/γ' interface model is shown in Fig. 1. The (002) atomic layer is taken as a coherent interface of the γ-Ni and γ'- Ni_3Al phase based on the experimental results reported by Harada et al. [34]. In order to investigate the effect of alloying element on the stability of γ/γ' interface, eight interfacial models with alloying elements, i.e., Ni(1), Ni(2), Ni(3), Al(4), Ni(5), Ni(6), Al(7) and Ni(8), are constructed. In these eight models, Ni atoms at Ni(1) site and Ni(2) site are located on the (002) and (001) atomic layer in the γ-Ni region, respectively. Ni atoms at Ni(3) site are located on the coherent (002) atomic layer (marked as (002) γ/γ' in Fig. 1). Al atoms at Al(4) and Al(7) site are located on the (001) atomic layer in the γ'-Ni3Al block (marked as (001) γ' in Fig. 1). Ni atoms at Ni(6) site are located on the (002) atomic layer in the γ'- Ni_3Al block. Ni atoms at Ni(5) and Ni(8) site are located on the (001) atomic layer in the γ'- Ni_3Al block.

For the sake of the symmetry in our calculations, the supercell is doped with alloying atom, i.e., one alloying atom for each interface. All atomic positions in the supercell with or without

alloying elements have been relaxed to their equilibrium positions according to the quantum-mechanical Hellmann–Feynman forces using conjugate-gradient algorithm.

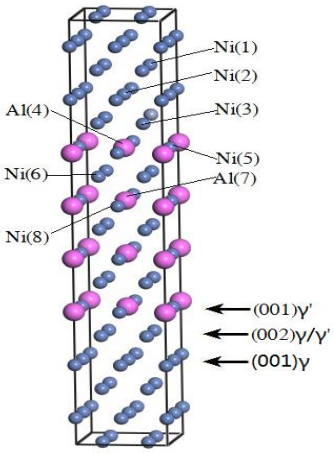

Fig. 1. The supercell model of the γ/γ′interface for calculation, in which the big and small balls denote Al and Ni atoms, respectively. (001)γ, (001)γ′ and (002)γ/γ′ represent the (001) atomic layer in γ-Ni, the (001) atomic layer in γ′-Ni_3Al block and the coherent γ/γ′ interfacial layer, respectively.

3. Results and discussion

3.1. Site preference and γ/γ' phase partitioning

In order to investigate the site preference of alloying elements at the γ-Ni and γ'-Ni3Al, the total energies of different models corresponding to Fig. 1 are calculated and are shown in Fig. 2. Clear model in Fig. 2 represents γ/γ' interfaces free of alloying atoms. It is interesting to find that with the Ru and W substitutions for all sites, the energies of the systems are lower than those of γ/γ' interfaces without alloying atoms, which may result in an improved microstructure stability of Ni-based single crystal superalloys. However, Ta and Co appear to give worse alloying stability effect than other alloying elements except for Al(4) and Al(7) sites at the coherent Ni_3Al phase. It is important to point out that the microstructures of Ni-based single crystal superalloys with Co, Ru, W and Ta substitutions for Al(4) and Al(7) sites are more stable than that of Ni-based single crystal superalloys free of alloying atoms. These results indicated that Co, Ru, W and Ta atoms have a preference for Al sites at the coherent Ni_3Al phase. Gong et al. [35] reported that the total energies of the γ/γ' interface with Re, Ru, Cr, Co, Mo, W, Ta atoms substitutions for Al and Ni sites from first-principles calculations were lower than that of clean γ/γ' interface. Geng et al. [12] concluded that only Mo and Ru have a tendency to stabilize the Ni_3Al phase in Mo, Rh, Ru, Ir, Pd, Os and Pt elements by first-principles calculations.

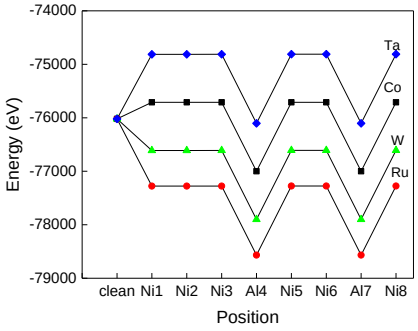

Fig. 2. The total energies of Ni-based single- crystal superalloys with or without alloying elements.

The site preference of the alloying elements in Ni-based single-crystal superalloys can be predicted by the binding energy of the supercell. The binding energy E_b is defined as [36]:

$$E_b = E_t - \sum_i E_{atom}(i) \quad (1)$$

where E_t is defined as the total energies of different models after the geometric relaxation, and $E_{atom}(i)$ is the energy of the free atom.

The binding energy (E_b) calculated for the supercells is shown as Fig. 3. It can be seen that E_b of Ni-based single crystal superalloys in the presence of Co, Ru, W and Ta atoms are lower than those of Ni-based single crystal superalloys without those atoms (Fig. 3 (a)). Thus, the substitutions for Co, Ru, W and Ta atoms can decrease E_b, which may result in an improved microstructure stability of Ni-based single crystal superalloys. For the same alloying element, it is also seen from the Fig. 3 that all binding energy of alloying elements at the γ'-A1(4) and γ'-Al (7) sites are the more negative. Thus, Co, Ru, W and Ta have a strongest preference for the γ'-Al(4) and γ'-Al(7) sites, which is consistent with the previous experimental results [37]. Then, those elements have a secondary preference for γ-Ni(1) and γ-Ni(2) sites, third-level preference for γ/γ'-Ni(3) site and the worst preference for γ'-Ni(5), γ'-Ni(6) and γ'-Ni(8) sites. Our results for the Ta and Ru site preference in Ni-based single crystal superalloys are the same as those of wang et al. [10], Geng et al. [12], and Jiang [38]. Moreover, it can be also seen from Fig. 3 (a), the binding energies of those alloying elements at the γ'-Al(4) site approach to that of γ'-Al(7) site. The same results were found for γ-Ni(1), γ-Ni(2) sites and for the γ'-Ni(5), γ'-Ni(6) γ'-Ni(8) sites. It is indicated that site preference of those alloying elements at the γ'-Al(4) and γ'-Al(7) sites, γ-Ni(1) and γ-Ni(2) sites, γ'-Ni(5) and γ'-Ni(6), γ'-Ni(8) sites are energetically equivalent.

For the same site of atoms in γ' or γ phase, we can also easily see that the binding energies show same trends according to the kinds of the alloying atoms added to Ni-based single crystal superalloys (Fig. 3 (b)). For γ-Ni(1), γ-Ni(2), γ'/γ-Ni(3), γ'-Al(4), γ'-Ni(5), γ'-Ni(6), γ'-Al(7) and γ'-Ni(8) sites, the binding energies decrease in the following order: Co < Ru <Ta < W. From these results we can see that W alloying elements have preferential site occupancy, while Co alloying elements have the weakest site occupancy tendency, regardless of γ phase, γ'/γ interface and γ' phase. Wen et al. [39] investigated the site preference of transition-metal elements in γ' phase from first-principles calculations. Cr, Mo, Re, Ta and W, in this order, strongly occupy the Al site in γ' phase.

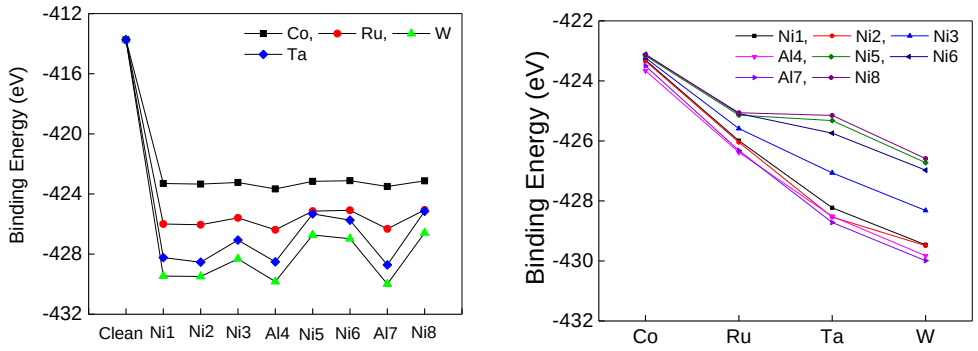

(a) *(b)*

Fig. 3. The binding energy of Ni-based single crystal superalloys with alloying elements.

In the γ' phase, the site preference of ternary alloying elements is governed directly by the differences in the substitution binding energies as:

$$\Delta E_{\text{sub}} = E_{\text{sub Al}}^{\text{M in } \gamma'} - E_{\text{sub Ni}}^{\text{M in } \gamma'} \tag{2}$$

where M represents alloying elements, $E_{\text{sub Al}}^{\text{M in } \gamma'}$ and $E_{\text{sub Ni}}^{\text{M in } \gamma'}$ are the binding energies of the M-alloying supercells for substituting Al or Ni in γ' phase, respectively.

Fig. 4 (a) presents first-principles calculated values of the site substitution behavior of ternary Co, Ru, Ta, and W to Ni_3Al. According to Fig. 4(a), Ru, W and Ta transition metal elements exhibit a strong Al site preference in the dilute ternary ordered L12 structure. The site occupancy behavior of transition metal elements in Ni_3Al shows that the preference for Al sites increases as the d-occupation number increases in the periodic table. The trend in occupancy agrees with previous theoretical values obtained by Ruban et al. [40] and Jiang et al. [41].

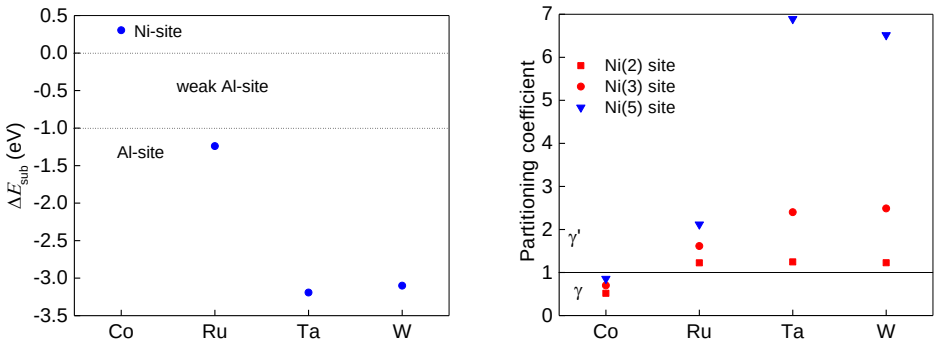

(a) *(b)*

Fig. 4. Site preference and γ/γ' phase partitioning. (a) the site preference behavior of Co, Ru, Ta, W transition metal elements in Ni_3Al based on first-principle calculated values according to Eq. (2), (b) partitioning coefficient of elements at 300K.

Numerically, the partitioning coefficient to characterize the phase preference of elements can be derived as [42]:

$$K_{\mathrm{M}}^{\gamma'/\gamma} = \exp\left(-\frac{E_{\text{sub Al}}^{\mathrm{M\ in\ }\gamma'} - E_{\text{sub Ni}}^{\mathrm{M\ in\ }\gamma}}{k_B T}\right) \tag{3}$$

where k_B is Boltzmann's constant and T is the absolute temperature. The partitioning tendency of transition metal elements in γ/γ' interface at 300K that is obtained by calculation is shown in Fig. 4(b). It is indicated that Co prefer the matrix phase, while Ru, W and Ta prefer the γ' phases. Mianroodi et al. [43] studied the role of Co in Ni-based superlloys by PFC simulations based a Ni-Al-Co embedded atom method (EAM) potential. The simulation results show that Co tends to segregate in both γ and γ' by replacing Ni atoms. As shown in Fig. 4(a), the substitution binding energies of Co, Ru, Ta, W at Al sublattice sites are 0.30 eV, -1.24 eV, -3.19 eV and -3.10 eV, respectively. Ta or W has stronger substitutional effect for Al sublattice sites of the γ' phases than Co or Ru. It implies that the additions of Ta or W can replace Ru, leading to a decrease of Ru content in the γ' phases.

3.2. Density of states

To obtain deeper insight into the alloying effect and partitioning behavior of Co, Ru, Ta and W in γ/γ' interface, the total density of states (TDOS) and the partial density of states (PDOS) of the γ/γ' interfaces with the Re, Ru, Cr, and W substitutions for γ-Ni(2), γ/γ'-Ni(3), γ'-Al(4) and γ'-Ni(5) sites were analyzed and are provided in Fig. 5 and Fig. 6. As shown in the TDOS analysis in Fig. 5, two sharp peaks located near -1.0 eV and -2.0 eV move toward the lower energy level for γ/γ' interface supercells due to the M-alloying addition. This result suggests that the alloying atoms Co, Ta and Co, W substituting the host atoms Ni at Ni(2) site and Ni at Ni(3) site, respectively, stabilize γ matrix phase, and the alloying atoms Ru, Ta, W and Co substituting the host atoms Al at Al(4) site and Ni at Ni(5) site, respectively, stabilize γ' phase.

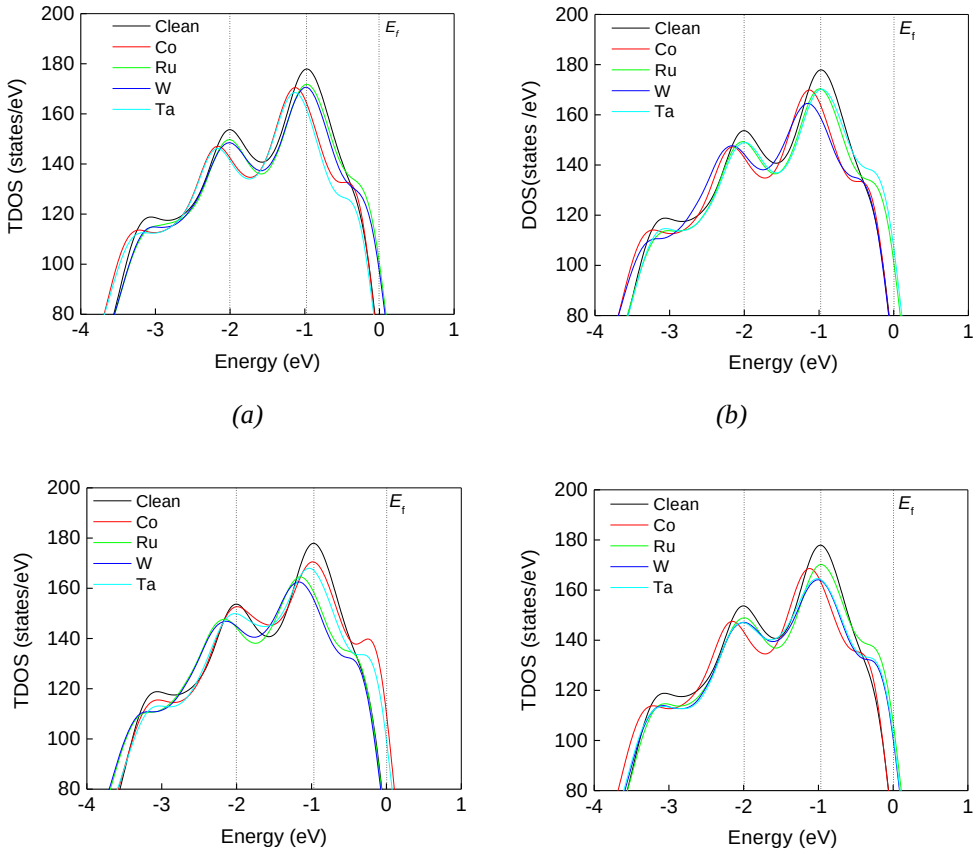

Fig. 5 Total density of states γ/γ' interface models without and with alloying elements for (a) Ni(2), (b) Ni(3), (c) Al(4) and (d) Ni(5) sites.

Fig. 6 shows the partial density of states (PDOS) of the γ/γ' interface models when Co, Ru, W and Ta atoms occupy Ni(2) site, Ni(3) site, Al(4) and Ni(5) site, respectively. The dotted line lied in zero-point energy represents the Fermi level (E_F). It can clearly be seen from Fig. 6 that several sharp bonding peaks are located near -5 and 0 eV, which shown there is hybridization between Co-3d, Ru-4d, Ta-5d, W-5d and Ni-3d, Al-3p orbitals. For the Co-doped γ/γ' interface models, we can see that from Fig. 6(a) there are three overlaps of the main peaks between the d state of Co located at Ni(2) site and Ni in γ in the higher energy region relative to that of Al, which shown there is d-d hybridization between Co-3d and Ni-3d orbitals. In contrast, PDOS of Al-3p and Al-2s orbitals locate in lower energy region, so this also makes the interaction between Co and Al atoms very weak. Moreover, it can be also seen from Fig. 6 (a) that there are no obvious d-d hybridization between the d states of Co located at Ni(3), Al(4), Ni(5) sites and Ni in γ/γ' interface, γ' phase, respectively. Those results show that Co atom prefers to occupy the Ni(2) site in γ phase. For the γ/γ' interface models doped with Ru, W and Ta, as shown in Fig. 6 (b), (c) and (d), respectively, there are d-d hybridization between Ru-4d, W-5d, Ta-5d orbitals located at Al4 site in γ' phase and Ni-3d orbitals in γ' phase. However, there are no obvious d-d hybridization between Ru-4d, W-5d, Ta-5d orbitals located at Ni2 site in γ phase, Ni3 site in γ/γ' interface, Ni(5) site in γ' phase and Ni-3d orbitals in γ' and γ phases. Moreover, there are also much bigger overlaps between Ru-4d, W-5d, Ta-5d orbitals and Al-3p orbital over the whole energy spectrum, thus there

are d-p hybridization between Ru-4d, W-5d, Ta-5d orbitals located at Al4 site in γ' phase and Al-3p orbital. It is indicated that Ru, W and Ta atoms prefer to occupy the Al site in γ' phase. The trend in occupancy agrees with previous theoretical values obtained by Ruban et al. [40] and Jiang et al. [41].

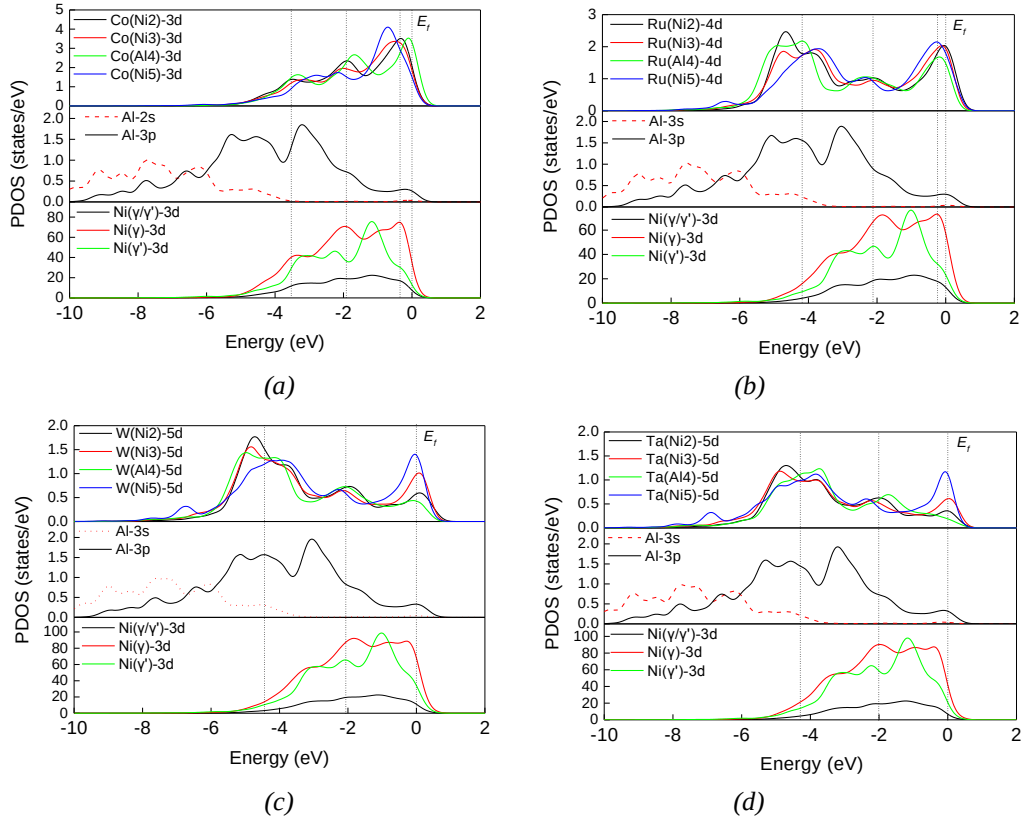

Fig. 6. The atomic partial density of states in the γ/γ' interface models with alloying elements, (a) Co, (b) Ru, (c) W, (d) Ta atom is substituted for Ni(2), Ni(3), Al(4) and Ni(5), respectively. The dotted lines imply the Fermi lever.

3.3. Electron density difference

To understand the interactions between the alloying element and its nearest neighbor host atoms further, we investigated the redistribution of electron density due to alloying element substitutions by electron density difference defined as

$$\Delta\rho(r) = \rho_{\text{cluster}}(r, X) - \rho_{\text{cluster}}(r) \tag{4}$$

where $\rho_{\text{cluster}}(r, \text{X})$ is the total electron density with X metal substitutions. Fig. 7 shows the electron density difference of the γ/γ' interface models doped with Co, Ru, W and Ta atoms substitution on (001) plane for Ni(2), Ni(3), Al(4) and Ni(5) sites. Electron density difference describes the direction and extent of electron transfer of atoms in γ/γ' interface models. The high electron density region (the deep color region) is correspond to core of the Ni, Al, Co, Ru, W and Ta atoms, and the range of electron density values is -0.07~0.15 e/Å^3 for γ/γ' interface models. The area of red stands for losing electrons and the area of blue stands for getting the electrons. It can be seen from Fig. 7 that the electrons have transferred between the adjacent atoms of Ni-(Al, Co, Ru, W

and Ta), it means that the Ni-Al is covalent bond, as well as Ni-Co, Al-Ru, Al-W and Al-Ta. Even though there are no obvious charge transfers between adjacent atoms Al-Al and Ni-Ni, a large number of electrons exist in the region between Al atoms and Ni atoms, meaning that covalent character exists in Al–Al and Ni-Ni bonds. Fig. 7(a) shows the electron density difference in the γ/γ' interface models doped with Co, Ru, W and Ta atoms substitution on (001) plane for Ni(2) sites. As expected, a strong bonding between Co and Ni atoms has been observed. This strong bonding is caused by the Co-3d/Ni-3d hybridization. The electrons density differences between Ni and Ru, W, Ta are close zero, indicating that the covalence of Ni-Ru, Ni-W, Ni-Ta are weaker than Ni-Co. This is consistent with the result of the site preference behavior in Fig. 4(a).

Fig. 7 (b) shows the electron density difference of the γ/γ' interface on the (001) plane. It can be seen that weaker enhancement of charge density between Co (Ru, W, Ta)-Ni atoms on the γ/γ' interface has been built up. As shown in Fig. 7 (c), the electron density difference for Co, Ru, W, Ta substitution for Al(4) site in γ' phase was shown. A significant anisotropic build-up of the directional d bonding charge at the Al(4) sites, which is caused mainly by the polarization of p electrons at the Al sites as a result of the p–d hybridization effect, along the Ni–Co (Ru, W, Ta) and Al–Ni directions, can be observed in Fig. 7 (c). It is interesting to note that Ru shows a similar charge distribution as W and Ta, except Co. This stronger bonding is obviously caused by the (Ru, W, Ta d)–(Ni d) hybridization than that of Co. The charge redistribution at Al sites, similar to Fig. 7 (b), is anisotropic and accumulated along Ni–Ru (W, Ta) direction. It is indicated that that Ru, W and Ta atoms prefer to occupy the Al site in γ' phase. The electron density difference for Co, Ru, W, Ta substitutions for Ni(5) site in γ' phase was shown in Fig. 7(d). It can be seen that the enhancement of charge density between Co (Ru, W, Ta) and Ni atoms is weaker than that between Al and Ni atoms in γ' phase. This shows that Co, Ru, W, Ta substitutions for Ni(5) site in γ' phase are unstable.

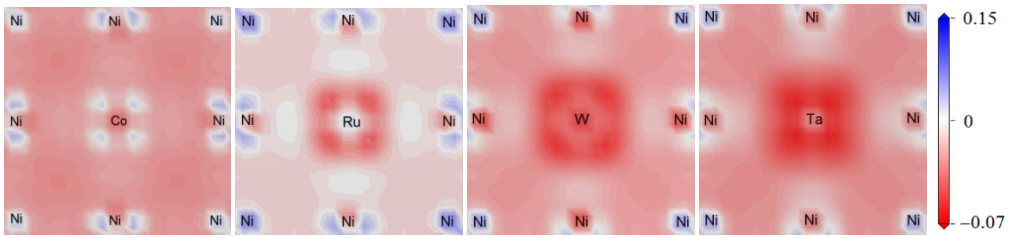

(a)

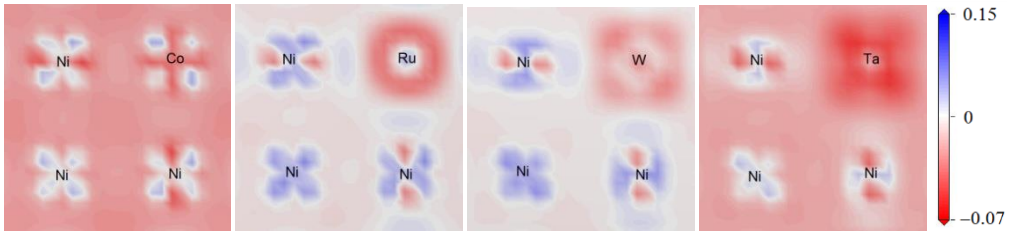

(b)

Fig. 7ab. The electron density difference contour of the γ/γ' interface with alloying elements on (001) plane for (a) Ni(2), (b) Ni(3), sites. Blue and red contour correspond to the gain and the loss of electrons, respectively.

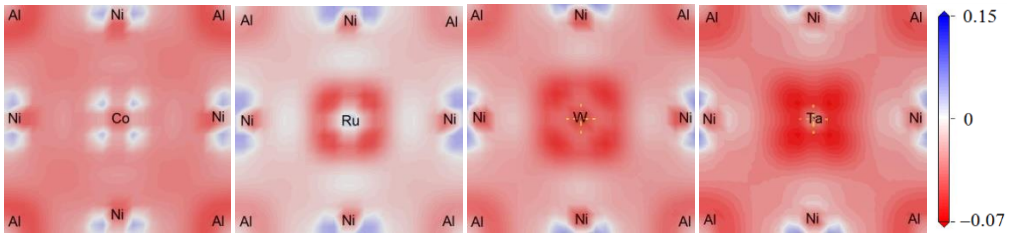

(c)

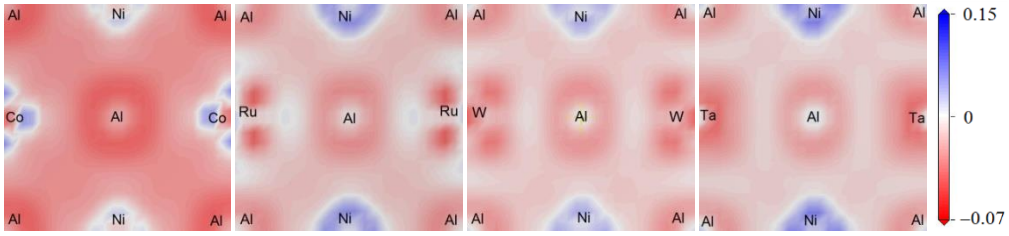

(d)

Fig. 7cd. The electron density difference contour of the γ/γ' interface with alloying elements on (001) plane for (c) Al(4) and (d) Ni(5) sites. Blue and red contour correspond to the gain and the loss of electrons, respectively.

4. Conclusion

Fully first principles ab itinio calculations have been performed to investigate the site preferences of alloying elements of Cr, Ru, W and Ta substitutions on the γ/γ' interface of Ni-based single-crystal superalloys. The calculation results show that Cr atom prefers to occupy a Ni site in γ phase, while Ru, W and Ta atoms prefer to occupy a Al site in γ' phase. When alloying elements replace the corresponding atoms from the γ/γ' interface, the total energy and binding energy decrease.

We also found that the electronic bonding mechanism of γ/γ' interface with the doped alloying elements can be summarized as the combination of d-d hybridization between Co-3d, d-p hybridization between Ru-4d, W-5d, Ta-5d orbitals located at Al4 site in γ' phase and Al-3p orbital and the electron charge transfer from Cr, Ru, W and Ta to Ni sites. The enhanced chemical bindings between alloying atoms and their neighbor host atoms are considered to be the main strengthening mechanism of the alloying elements in γ/γ' interface of Ni-based single-crystal superalloys.

Acknowledgements

This work was supported by the National Natural Science Foundation of China (No. 51871221), Science and Technology Project of Deyang (No.2018CKJ001), Shenyang Young and Middle-aged Science and Technology Innovation Talents Project (RC200355) in Liaoning Province, China.

References

[1] C.T. Sims (ed.), Superalloys II (Wiley, New York, 1987).
[2] J. H. Xu, A. J. Freeman, Phys. Rev. B **36**, 4186 (1987).
[3] B. I. Min, H. J. F. Jansen, Phys. Rev. B **37**, 6757 (1988).
[4] J. H. Xu, B. I. Min, A. J. Freeman, T. Oguchi, Phys. Rev. B **41**, 5010 (1990).
[5] J. C. Cao, F. S. Liu, C. Y. Wang, J. Phys. F **18**, 1839 (1988).
[6] J. L. Yang, C. Y. Xiao, S. D. Xia, K. L. Wang, J. Phys: Condens. Matter **5**, 6653 (1993).
[7] H. Marcel, F. Sluiter, Y. Kawazoe, Phys. Rev. B **51**, 4062 (1995).
[8] A. V. Ruban, H. L. Skriver, Phys. Rev. B **55**, 856 (1997).
[9] J. Shen, Y. Wang, N. X. Chen, Y. Wu, Progr. Nat. Sci. **10**, 457 (2000).
[10] S. Y. Wang, C. Y. Wang, J. H. Sun, W. H. Duan, D. L. Zhao, Phys. Rev. B **65**, 035101 (2001).
[11] N. Garimella, M. Ode, M. Ikeda, H. Murakami, Y. H. Sohn, Intermetallics **16**, 1095 (2008).
[12] C. Y. Geng, C. Y. Wang, T. Yu, Acta Mater. **52**, 5427 (2004).
[13] Q. Wu, S. S. Li, Comp. Mater. Sci. **53**, 436 (2012).
[14] H. E. Collins, Metall. Trans. A **5**, 189 (1974).
[15] S. M. Li, W. Du, J. Zhang, Acta Metall. Sin. **8**, 1195 (2002).
[16] G. E. Fuchs, Mater. Sci. Eng. A **300**, 52 (2001).
[17] M. J. Donachie, Superalloys: A Technical Guide, 2nd edn. (ASM International, 2002).
[18] R. C. Reed, The Superalloys Fundamentals and Applications (Cambridge University Press, Cambridge, 2006).
[19] P. Caron, O. Lavigne, Aersosp. Lab. **3**, 1 (2011).
[20] A. C. Yeh, S. Tin, Metall. Mater. Trans. A **37**, 2621 (2006).
[21] L. J. Carroll, Q. Feng, J. F. Mansfield, T. M. Pollock, Metall. Mater. Trans. A **37**, 2927 (2006).
[22] A. Sato, H. Harada, T. Yokokawa, T. Murakumo, Y. Koizumi, T. Kobayashi, H. Imai, Scripta Mater. **54**, 1679 (2006).
[23] R. C. Reed, A. C. Yeh, S. Tin, S. S. Babu, M. K. Miller, Scr. Mater. **51**, 327 (2004).
[24] T. Yokokawa, M. Osawa, M. Osawa, K. Nishida, Y. Koizumi, T. Kobayashi, H. Harada, J. Japan Inst. Metals **66**, 873 (2002).
[25] Y. Zhou, Z. Mao, C. Booth-Morrison, D. N. Seidman, Appl. Phys. Lett. **93**, 171905 (2008).
[26] Y. Amouyal, Z. Mao, C. Booth-Morrison, D.N. Seidman, Appl. Phys. Lett. **94**, 041917 (2009).
[27] S. Ma, J. Zhang, Progress in Natural Science: Materials International, **27**, 636 (2017).
[28] B. Wang, J. Zhang, T. Huang, H. Su, Z. Li, L. Liu, H. Fu, J. Mater. Res. **33**, 3381 (2016).
[29] W. Gong, W. Zhao, N. Miao, J. Zhou, Z. Sun, S. Li, S. Gong, Comp. Mater. Sci. **144**, 23 (2018).
[30] W. Zhao, Z. Sun, S. Gong, Intermetallics **65**, 75 (2015).
[31] W. Kohn, L. J. Sham, Phys. Rev. A. **140**, 1133 (1965).
[32] http://www.pwscf.org.
[33] H. J. Monkhorst, J. D. Pack, Phys. Rev. B **13**, 5188 (1976).
[34] H. Harada, A. Ishida, H. K. D. H. Bhadeshia, M. Yamazaki, Appl. Surf. Sci. **67**, 299 (1993).
[35] X. F. Gong, G. X. Yang, Y. H. Fu, Y. Q. Xie, J. Zhuang, X. J. Ning, Comp. Mater. Sci. **47**,

320 (2009).
[36] S.Y. Ma, J.X. Zhang, Philos. Mag. Lett. **95**, 253 (2016).
[37] A. P. Ofori, C. J. Humphreys, S. Tin, C. N. Jones, in: K.A. Green, T.M. Pollock, H. Harada, T. E. Howson, R.C. Reed, J.J. Schirra, S. Walston (eds.), Superalloy (TMS, Warrendale, PA, 2004), p. 787.
[38] C. Jiang, D.J. Sordelet, B. Gleeson, Acta Materialia **54**, 1147 (2006).
[39] M. Wen, C.Y. Wang, Phys. Rev. B **97**, 024101 (2018).
[40] A.V. Ruban, H. L. Skrive, Phys. Rev. B **55**, 856 (1997).
[41] C. Jiang, B. Gleeson, Scripta Materialia **55**, 433 (2006).
[42] Y. Amouyal, Z. Mao, D. N. Seidman, Acta Materialia **74**, 296 (2014).
[43] J. R. Mianroodi, P. Shanthraj, P. Kontis, J. Cormier, B. Gault, B. Svendsen, D. Raabe, Acta Materialia **175**, 250 (2019).